MOLECULAR
METABOLISM

Tyrosine-phosphorylated DNER sensitizes insulin signaling in hepatic gluconeogenesis by inducing proteasomal degradation of TRB3

Junfeng Li[1],[*], **Yan Huang**[1], **Xinyu Yang**[2], **Yuli Cai**[1], **Ye Wang**[1], **Wenling Dai**[1], **Liu Jiang**[1], **Changhua Wang**[2], **Zhongyuan Wen**[1],[**]

ABSTRACT

Objective: Hepatic insulin resistance, which leads to increased hepatic gluconeogenesis, is a major contributor to fasting hyperglycemia in type 2 diabetes mellitus (T2DM). However, the mechanism of impaired insulin-dependent suppression of hepatic gluconeogenesis remains elusive. Delta/Notch-like epidermal growth factor (EGF)-related receptor (DNER), firstly described as a neuron-specific Notch ligand, has been recently identified as a susceptibility gene for T2DM through genome-wide association studies. We herein investigated whether DNER regulates hepatic gluconeogenesis and whether this is mediated by enhanced insulin signaling.

Methods: The association between DNER, tribbles homolog 3 (TRB3) and Akt signaling was evaluated in C57BL/6J, *ob/ob* and *db/db* mice by western blot analysis. DNER loss-of-function and gain-of-function in hepatic gluconeogenesis were analyzed by western blot analysis, quantitative real-time PCR, glucose uptake and output assay in AML-12 cells and partially validated in primary mouse hepatocytes. Hepatic DNER knockdown mice were generated by tail vein injection of adenovirus to confirm the effects of DNER *in vivo*. The interaction between DNER and TRB3 was investigated by rescue experiments, cycloheximide chase analysis, co-immunoprecipitation and immunofluorescence. The potential insulin-stimulated phosphorylation sites of DNER were determined by co-immunoprecipitation, LC-MS/MS analysis and site-specific mutagenesis.

Results: Here we show that DNER enhanced hepatic insulin signaling in gluconeogenesis by inhibiting TRB3, an endogenous Akt inhibitor, through the ubiquitin-proteasome degradation pathway. In AML-12 hepatocytes, insulin-stimulated activation of Akt and suppression of gluconeogenesis are attenuated by DNER knockdown, but potentiated by DNER over-expression. In C57BL/6J mice, hepatic DNER knockdown is accompanied by impaired glucose and pyruvate tolerance. Furthermore, the *in vitro* effects of DNER knockdown or over-expression on both Akt activity and hepatic gluconeogenesis can be rescued by TRB3 knockdown or over-expression, respectively. In response to insulin stimulation, DNER interacted directly with insulin receptor and was phosphorylated at Tyr^{677}. This site-specific phosphorylation is essential for DNER to upregulate Akt activity and then downregulate G6Pase and PEPCK expression, by interacting with TRB3 directly and inducing TRB3 proteasome-dependent degradation.

Conclusions: Taken together, the crosstalk between insulin-Akt and DNER-TRB3 pathways represents a previously unrecognized mechanism by which insulin regulates hepatic gluconeogenesis.

1. INTRODUCTION

The abnormally increased hepatic glucose production (HGP) and insensitivity of this parameter to insulin are hallmarks of type 2 diabetes mellitus (T2DM) [1,2]. Gluconeogenesis has been identified as the primary source of excessive HGP in individuals with T2DM, while glycogenolysis was found not to contribute [1—3]. In hepatic insulin-resistant state, gluconeogenesis cannot be appropriately suppressed by insulin, which results in increased HGP and is the major contributor to fasting hyperglycemia, but the underlying signaling mechanism remains to be fully explored.

Hepatic gluconeogenesis is a complex process, largely controlled by transcriptional regulation of key rate-limiting enzymes, specifically glucose-6-phosphatase (G6Pase) and phosphoenolpyruvate

[1]Department of Endocrinology, Renmin Hospital of Wuhan University, Wuhan 430060, China [2]Department of Pathology & Pathophysiology, Wuhan University School of Basic Medical Sciences, Wuhan 430071, China

*Corresponding author.

**Corresponding author.

E-mails: junfeng.li@whu.edu.cn (J. Li), huangyan17@qq.com (Y. Huang), 2021203010054@whu.edu.cn (X. Yang), cyl-07@163.com (Y. Cai), wye2018@whu.edu.cn (Y. Wang), 316084554@qq.com (W. Dai), jiang_liu1001@163.com (L. Jiang), chwang0525@whu.edu.cn (C. Wang), zhongyuan.wen@whu.edu.cn (Z. Wen).

carboxykinase (PEPCK) [3]. Insulin is a major hormone regulating hepatic gluconeogenesis via the phosphoinositide 3-kinase (PI3K)/Akt (also called protein kinase B) signaling pathway. Forkhead box O1 (FoxO1), a member of the forkhead family of transcription factors, is a particularly well-characterized Akt target, with important physiological functions involving gene expression of G6Pase and PEPCK in hepatocytes [1,3]. Under physiological conditions, phosphorylation of FoxO1 by Akt leads to its inactivation through translocation from nucleus to cytoplasm [1—3]. In insulin-resistant status, decreased Akt-mediated inactivation of hepatic FoxO1 increases G6Pase and PEPCK expression, thereby inducing hepatic gluconeogenesis and fasting hyperglycemia in patients with T2DM [1—3].

The importance of maintaining normal hepatic gluconeogenic rates in the management of T2DM has been underscored by current therapeutical approaches to suppression of gluconeogenesis including intermediate-acting insulin given at bedtime and metformin [4]. Therefore, exploring new regulatory pathways which can sensitize insulin action in hepatic gluconeogenesis might inform potential novel therapeutic strategies for T2DM, one of the greatest global health challenges.

Delta/Notch-like epidermal growth factor (EGF)-related receptor (DNER, also named BET and HE60), identified initially as a neuron-specific Notch ligand mediating neuron—glia interaction during astrocytogenesis [5], is also expressed in a variety of cells including glioblastoma-derived neoplastic stem-like cells, human adipose tissue-derived mesenchymal stem cells, hair cells in inner ear and C2C12 myoblasts, where it played an important role in cell differentiation and proliferation [5—8]. In addition, we have demonstrated that phosphorylated DNER can interact with Girdin to activate PI3K/Akt signaling pathway in breast cancer cells [9]. It is noteworthy that *DNER* was recently identified as a T2DM-susceptibility gene in American Indians and Chinese Han populations, and the diabetes risk allele at rs1861612 was associated with increased homeostasis model assessment of insulin resistance [10,11]. These studies suggest a potential contribution of DNER in insulin signaling pathway. Meanwhile, Notch1, a member of the Notch receptor family, which directly binds with DNER in Purkinje neurons and C2C12 myoblasts [5], can regulate hepatic G6Pase expression in a FoxO1-dependent manner [12,13]. Therefore, we speculate that DNER may play a role in hepatic insulin signaling and gluconeogenesis.

In this study, we showed that DNER enhanced insulin signaling in hepatic gluconeogenesis by inhibiting tribbles homolog 3 (TRB3), an endogenous Akt inhibitor [14], through the ubiquitin-proteasome degradation pathway. We found that DNER was phosphorylated in response to insulin stimulation and interacted directly with insulin receptor. Furthermore, we demonstrated that phosphorylation at Tyr^{677} is critical for DNER to mediate the crosstalk between insulin and DNER-TRB3 pathways. Our results uncovered the role of DNER in hepatic gluconeogenesis and its insulin-sensitizing effect.

2. MATERIALS AND METHODS

2.1. Animals procedures
Female C57BL/6J, *db/db* and *ob/ob* mice at 7-week of age were purchased from the Model Animal Research Center of Nanjing University and housed for 1-week period of adaptation, in a 24 °C, 12-h light/dark cycle condition with free access to water and standard chow (20% kcal protein, 10% kcal fat and 70% kcal carbohydrates) according to guidelines approved by the Animal Care and Use Committee of Wuhan University. Two studies were performed as below.

The first study explored the potential association between DNER and PI3K/Akt signaling in insulin target tissues. Six C57BL/6J, six *db/db* and six *ob/ob* mice were sacrificed at 8-week of age. Livers, skeletal muscles as well as visceral (epididymal) adipose tissues were harvested, and western blot was performed to measure the protein levels of DNER, TRB3 and Akt signaling molecules.

The second study investigated the effects of hepatic DNER knockdown in C57BL/6J mice. Twenty mice at 8-week of age were randomized into two groups (n = 10 per group). Two tail-vein injections of adenovirus packaging short hairpin RNA (shRNA) against DNER (DNER shRNA group) or nonsense shRNA as control (DNER scramble group) were administered at 1-week intervals. Five days after the second injection of adenoviruses, the mice were fasting and subjected to glucose and pyruvate tolerance tests. Subsequently, blood samples were collected for biochemical analysis as described in SI Experimental Procedures, and then mice were sacrificed and liver was harvested for experimental measurements.

2.2. Cell culture and treatment
AML-12 cells, an immortalized normal mouse hepatocyte cell line, were obtained from American Type Culture Collection (ATCC, Rockville, MD, USA, CRL-2254) and cultured in DMEM/F12 medium. Before experiments, AML-12 cells were plated at subconfluency and incubated for 6 h in serum-free medium. Primary mouse hepatocytes were isolated from C57BL/6J mice by two-step collagenase perfusion method with some modifications [15]. The detailed primary hepatocytes isolation, cell culture, treatment and reagents used are described in SI Experimental Procedures.

2.3. Plasmid construction and adenovirus infection
To construct adenoviral vector for over-expression of DNER, cDNA encoding full-length HA-tagged DNER was linked to the adenovirus shuttle vector pENTER, and subcloned into pAD-FH adenoviral backbone vector through recombination in *Escherichia coli*, as described in SI Experimental Procedures. Efficacy of DNER over-expression was determined in Supplementary Figure 1. The point mutant DNER construct (Tyr^{677} to Ala) were generated by PCR using full-length DNER cDNA as template (Supplementary Figure 2). Adenovirus expressing only HA was used as control.

Adenovirus vectors containing short hairpin RNA (pAdM-U6-shRNA) against DNER and scrambled shRNA control were purchased from Vigene Biosciences, and screened in a pilot study for knockdown efficiency and specificity in AML-12 hepatocytes and C57BL/6J mice (Supplementary Figure 3).

To over-express or knock down TRB3, AML-12 cells were transfected with the pcDNA3.1-3xFlag-TRB3 plasmid with empty vector as control constructed by YouBio (Changsha, Hunan, China), or the pLKO.1-TRC plasmid containing shRNA against TRB3 with nonsense shRNA as control constructed by Sangong Biotechnology (Shanghai, China). Efficacy of TRB3 over-expression or knockdown were determined in Supplementary Figure 4.

2.4. Small interfering RNAs and transfection
AML-12 cells were transfected with siRNA specific to Girdin or scrambled control synthesized by Genechem (Shanghai, China), as described in SI Experimental Procedures. Knockdown efficiency was assessed by quantitative PCR (Supplementary Figure 5).

2.5. Glucose output and uptake assay
For the glucose output assay, hepatocytes were washed three times with PBS and then transferred to glucose-free and phenol red-free

DMEM with 20 mM sodium lactate and 2 mM sodium pyruvate for 6 h as described in SI Experimental Procedures. Supernatants were used for measurements of glucose concentration, which was normalized to the total amount of protein in each well.

Glucose uptake was determined using Glucose Uptake Colorimetric Assay kit (Abcam, Cambridge, MA, USA) according to the manufacturer's protocol, as described in SI Experimental Procedures. All glucose output and uptake measurements were performed in triplicate.

2.6. RNA isolation and quantitative real-time PCR

RNA from AML-12 cells and mouse liver tissues was isolated using TRIzol reagent, reverse transcribed to complementary DNA and quantified with Real-Time PCR system, as described in SI Experimental Procedures. GAPDH was used as an internal control for normalization. Primer sequences are provided in the Supplementary Table 1.

2.7. Western blot analysis

Western blot was performed as previously described [9,16]. AML-12 cells or mouse liver tissues were lysed in RIPA lysis buffer. The proteins were loaded, separated by SDS-PAGE gel, transferred to nitrocellulose membranes and detected with specific antibodies. Protein bands densities were quantified using Glyko BandScan software, and data were normalized to control. Antibodies used are listed in Supplementary Table 2.

2.8. Cell fractionation

After treatments, AML-12 cells were washed and harvested in cold PBS. The nuclear, cytoplasmic and membrane proteins were separated by using the Nuclear and Cytoplasmic Protein Extraction Kit (Beyotime, Shanghai, China) and the Membrane and Cytosol Protein Extraction kit (Beyotime) according to the manufacturer's protocol. The anti-Na/K-ATPase as a membrane marker, anti-GAPDH as a cytoplasmic marker and anti-Histone 3 as a nuclear marker were used as loading controls.

2.9. Co-immunoprecipitation analysis

Co-immunoprecipitation (Co-IP) studies were performed in lysates of AML-12 cells and mouse liver tissues as described previously [9,16], using anti-Insulin Receptor β, anti-TRB3 or anti-HA antibodies (Supplementary Table 2) at 4 °C followed by immunoprecipitation using protein A beads. The antigen—antibody complex was eluted from the beads and analyzed by western blot, as described in SI Experimental Procedures.

2.10. Phosphorylated peptide enrichment and LC-MS/MS analysis

Three biological replicates of AML-12 cells transfected with HA-tagged DNER and stimulated with or without 100 nM insulin for 10 min were prepared for LC-MS/MS Analysis, as described in SI Experimental Procedures.

2.11. Immunohistochemistry and immunofluorescence

Liver tissues of C57BL/6J mice with or without hepatic DNER knockdown and AML-12 cells transfected with HA-tagged DNER were fixed for downstream staining and imaging, as described in SI Experimental Procedures.

2.12. Glucose and pyruvate tolerance tests

For oral glucose tolerance test (OGTT), mice were fasted 12 h, followed by gavage with glucose (2 g/kg of body weight). For pyruvate tolerance test (PTT), 6 h fasted mice received an intraperitoneal sodium pyruvate (2 g/kg of body weight) injection. Blood samples of mice were collected from the tail vein at 0, 15, 30, 45, 60, 90 and 120 min after glucose or pyruvate administration, and determined using a portable glucometer (Bayer, German).

2.13. Serum alanine and aspartate aminotransferase

Mice liver function in this study was assessed by measuring the concentrations of alanine aminotransferase (ALT) and aspartate aminotransferase (AST) in serum using a BX3010 automatic biochemical analyzer (Sysmex, Kobe, Japan) according to the manufacturer's instructions.

2.14. Statistical analysis

Data were presented as mean $\pm$ SE of independent experiments, and analyzed either by unpaired Student t test or One-way ANOVA with Tukey post-hoc test as appropriate, using Statistical Product and Service Solutions (SPSS) version 19.0. All tests were two-sided, with a p value < 0.05 considered statistically significant.

3. RESULTS

3.1. DNER and phosphorylated Akt are downregulated while TRB3 is upregulated in insulin target tissues of *ob/ob* and *db/db* mice, compared with that in C57BL/6J mice

To explore the role of DNER in insulin signaling pathway, we first compared the protein levels of DNER, TRB3 and phosphorylated Akt in insulin target tissues of age- and gender-matched C57BL/6J, *ob/ob* and *db/db* mice (Figure 1).

The protein level of DNER in the liver (Figure 1A), skeletal muscle (Figure 1B) and visceral (epididymal) adipose tissues (Figure 1C) of *ob/ob* and *db/db* mice were significantly lower than that of C57BL/6J mice. In contrast, the protein level of TRB3 in the liver, skeletal muscle and visceral adipose tissues of *ob/ob* and *db/db* mice were significantly higher than that of C57BL/6J mice. Consistent with these, the Akt phosphorylation in the liver, skeletal muscle and visceral adipose tissues of C57BL/6J mice were significantly higher than that of *ob/ob* and *db/db* mice.

These results showed that DNER protein level was positively related to Akt phosphorylation, while TRB3 protein level was negatively related to Akt phosphorylation. Furthermore, the DNER expression and Akt activation were downregulated, whereas TRB3 expression was upregulated in insulin-resistant state.

3.2. DNER knockdown impaired insulin signaling in hepatic gluconeogenesis *in vitro* and *in vivo*

To investigate the role of DNER in regulating hepatic gluconeogenesis *in vitro*, we employed the adenoviral delivery system for knockdown of DNER protein in AML-12 cells. The DNER protein level was decreased by approximately 65% in AML-12 cells infected with adenovirus that encodes a shRNA specific to the DNER gene, compared with the cells infected with adenovirus encoding a scrambled control (Supplementary Figure 3).

Knockdown of DNER expression attenuated phosphorylation of Akt, and consequently reduced the phosphorylation of FoxO1, resulting in increased gluconeogenic genes (G6Pase and PEPCK) expression under both basal and insulin-stimulated conditions (Figure 2A—C). These changes during DNER knockdown was accompanied by decreased 2-DG uptake (Supplementary Figure 6), increased glucose production (Figure 2D) and reduced phosphorylation of GSK3α/β (Figure 2A,B), another Akt downstream targets besides FoxO1.

Although adenovirus-mediated knockdown of DNER impaired insulin-evoked Akt activation (Figure 2A,B), it had no obvious effect on
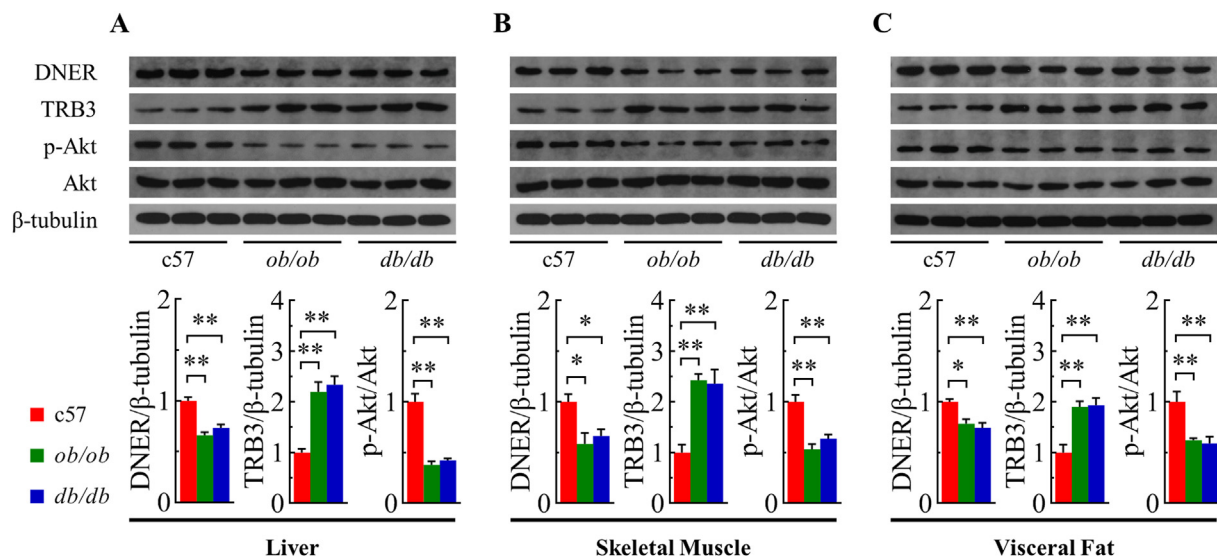
Figure 1: The protein levels of DNER−TRB3−p-Akt in the liver, skeletal muscle and visceral adipose tissues of C57BL/6J, *ob/ob* and *db/db* mice. (A) Livers, (B) skeletal muscles as well as (C) visceral (epididymal) adipose tissues of eight-week-old female c57 (C57BL/6J), *ob/ob* and *db/db* mice were harvested, and subjected to western blot analysis to measure the protein levels of DNER, TRB3 and p-Akt signaling molecules. Data were normalized to control (c57 group) and expressed as mean ± SE. n = 6. *, $p < 0.05$; **, $p < 0.01$.

either the protein abundance or the phosphorylation of insulin receptor and PDK1 (Figure 2A,B), two upstream signaling molecules of Akt.

In addition, shRNA-mediated reduction of DNER expression did not affect TRB3 gene expression (Figure 2C,I), but increased TRB3 protein expression (Figure 2A, B, G and H), suggesting that DNER may regulate the stability of TRB3 protein.

To investigate the effects of DNER on hepatic insulin sensitivity *in vivo*, we injected C57BL/6J mice with adenovirus encoding DNER-specific siRNA to reduce its expression in the liver. Western blot analysis showed the protein abundance of DNER was decreased by approximately 70% in the liver after injection with adenoviruses compared to the scrambled control group (Supplementary Figure 3).

Adenovirus-mediated knockdown of DNER *in vivo* had no obvious effect on food intake, body weight gain and liver function as assessed by serum ALT/AST levels (Supplementary Figure 7), or on hepatocyte morphology evaluated by H&E staining (Supplementary Figure 8), but significantly increased fasting blood glucose (Supplementary Figure 7). Glucose and pyruvate tolerance tests performed from day 6 after the second adenoviral injection showed significantly impaired glucose tolerance (Figure 2E) and excessive pyruvate-glucose conversion (Figure 2F), as evidenced by a much larger area under the glucose curve compared to the scrambled control.

These changes during DNER knockdown *in vivo* was accompanied at a molecular level by increased TRB3 protein expression, attenuated phosphorylation of Akt and its two downstream targets GSK3α/β and FoxO1, leading to increased gene and protein level of G6Pase and PEPCK (Figure 2G−I), a finding consistent with the observation in AML-12 hepatocytes.

3.3. The potentiating effect of DNER on hepatic insulin signaling is Notch1-and Girdin-independent

To examine whether the potentiating effect of DNER on hepatic insulin signaling is through the modulation of Notch1 pathway, we conducted quantitative real-time PCR analysis in AML-12 cells with DNER over-expression or knockdown, and then treated with 20 μM DAPT for 12 h, followed with 100 nM insulin for 6 h. Over-expression of DNER markedly increased the magnitude of insulin-mediated suppression of gluconeogenic genes (G6Pase and PEPCK) expression and vice versa, which cannot be blocked by the Notch1 inhibitor DAPT (Figure 3A). To further confirm the above findings, we also examined the effect of DNER over-expression on Notch1 signaling pathway using western blot analysis in AML-12 cells. DNER can neither regulate the expression of Notch1 nor its downstream target proteins such as HES1 and HEY1 (Figure 3B,C). Meanwhile, we performed Co-IP experiments and the results showed no interaction between DNER and Notch1 (Figure 6D). These findings indicate that the effect of DNER on hepatic insulin signaling is independent of Notch1.

To investigate whether Girdin participates in DNER-mediated hepatic gluconeogenesis, we performed quantitative real-time PCR and western blot analysis in AML-12 cells stimulated with 100 nM insulin for 6 h. Over-expression or knockdown of DNER had no effect on the gene and protein levels of Girdin (Figure 3D−F). Moreover, the role of DNER in reducing the expression of hepatic gluconeogenic genes (G6Pase and PEPCK) remained in a Girdin-silenced context (Figure 3G). We further conducted Co-IP experiments to examine the interplay between DNER and Girdin, and the results showed no interaction between DNER and Girdin (Figure 6D). These findings suggest that DNER regulates hepatic gluconeogenesis through a Girdin-independent pathway.

3.4. DNER negatively regulates hepatic gluconeogenesis through TRB3-Akt signaling pathway

To elucidate whether DNER negatively regulates hepatic gluconeogenesis through TRB3-Akt signaling pathway, we performed western blot analysis in AML-12 cells co-transfected with DNER and/or TRB3. Over-expression of DNER significantly enhanced insulin-stimulated phosphorylation of Akt and its two downstream signaling molecules FoxO1 and GSK3α/β (Figure 4A,B), consequently resulting in decreased expression of G6Pase and PEPCK (Figure 4C,D) and reduced glucose production (Supplementary Figure 6). On the contrary, knockdown of DNER attenuated insulin-stimulated Akt-FoxO1/GSK3α/β phosphorylation, increased G6Pase and PEPCK expression (Figure 4A−D) and promoted glucose production (Figure 2D). Moreover, the improved or
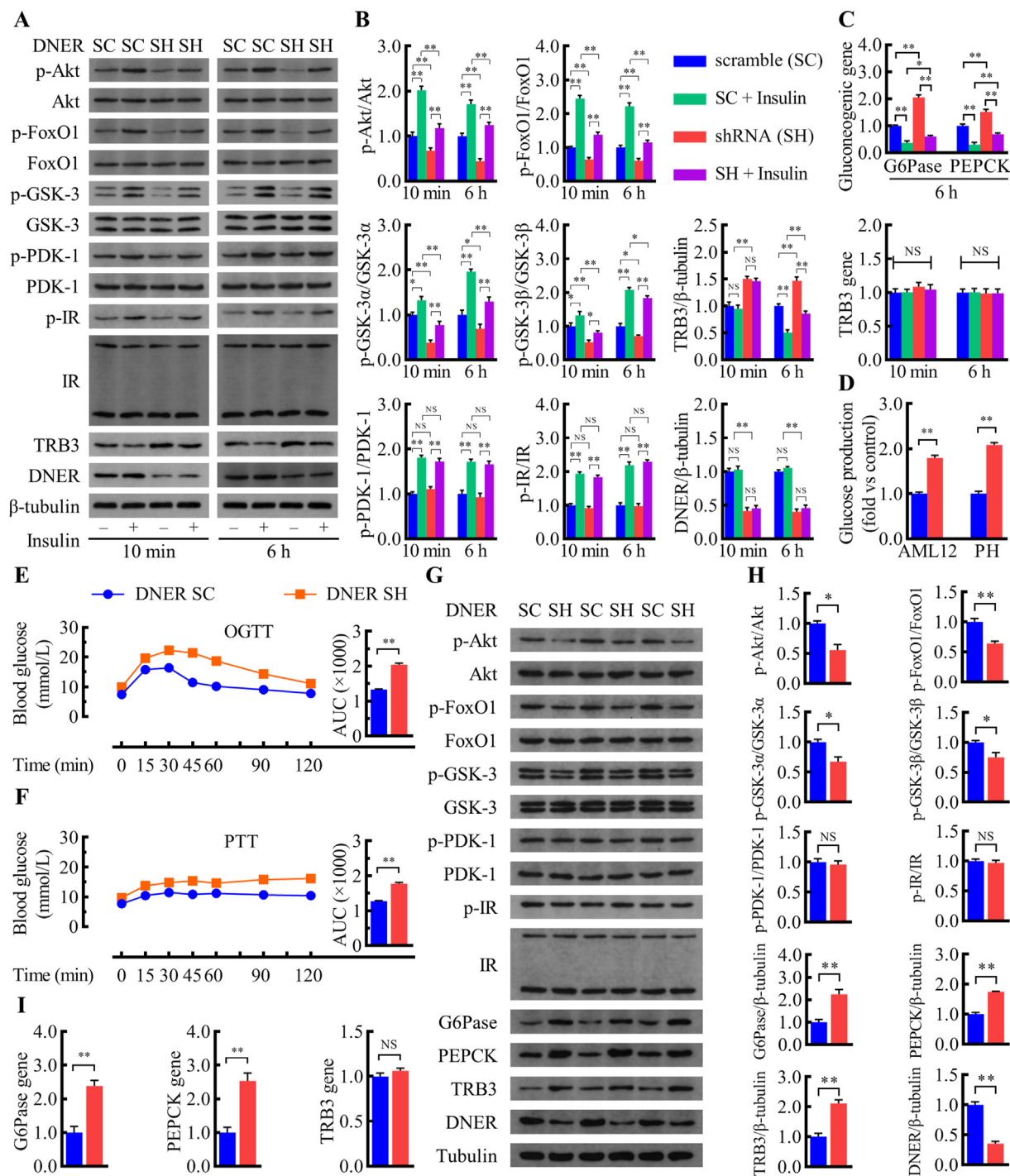
Figure 2: Suppression of DNER expression by shRNA decreases insulin-evoked activation of the Akt—FoxO1—G6Pase/PEPCK signaling pathway in AML-12 cells and induces hyperglycemia in C57BL/6J mice. (A—D) AML-12 cells transfected with adenovirus encoding DNER-specific shRNA or scrambled control were treated with 100 nM insulin for 10 min or 6 h: (A—B) Total cell lysates were subjected to western blot analysis using antibodies as indicated. (C) The mRNA expression of G6Pase, PEPCK and TRB3 were quantified by real-time PCR, with GAPDH serving as an internal control for normalization. (D) Glucose output assay was performed in AML-12 cells and primary mouse hepatocytes (PH) transfected with adenovirus encoding DNER-specific shRNA or scrambled control. n = 6. (E—I) Eight-week-old C57BL/6J female mice were treated with adenoviruses encoding DNER shRNA or scrambled control by two tail-vein injection: (E—F) Glucose concentrations during OGTT (E) or PTT (F) and area under the curve (AUC) for OGTT or PTT in mice five days after the second tail vein injection. n = 10. (G—I) Liver tissues of mice were harvested for (G—H) western blot analysis using antibodies as indicated and (I) real-time PCR to detect mRNA expression of G6Pase, PEPCK and TRB3, with GAPDH serving as an internal control for normalization. n = 3. Data were normalized to scrambled control (SC group; B, C, H and I) and expressed as mean ± SE. *, p < 0.05; **, p < 0.01; NS, not statistically significant. IR, insulin receptor; p-IR, phosphorylated IR. SC, DNER scrambled control group; SH, DNER-specific shRNA group.
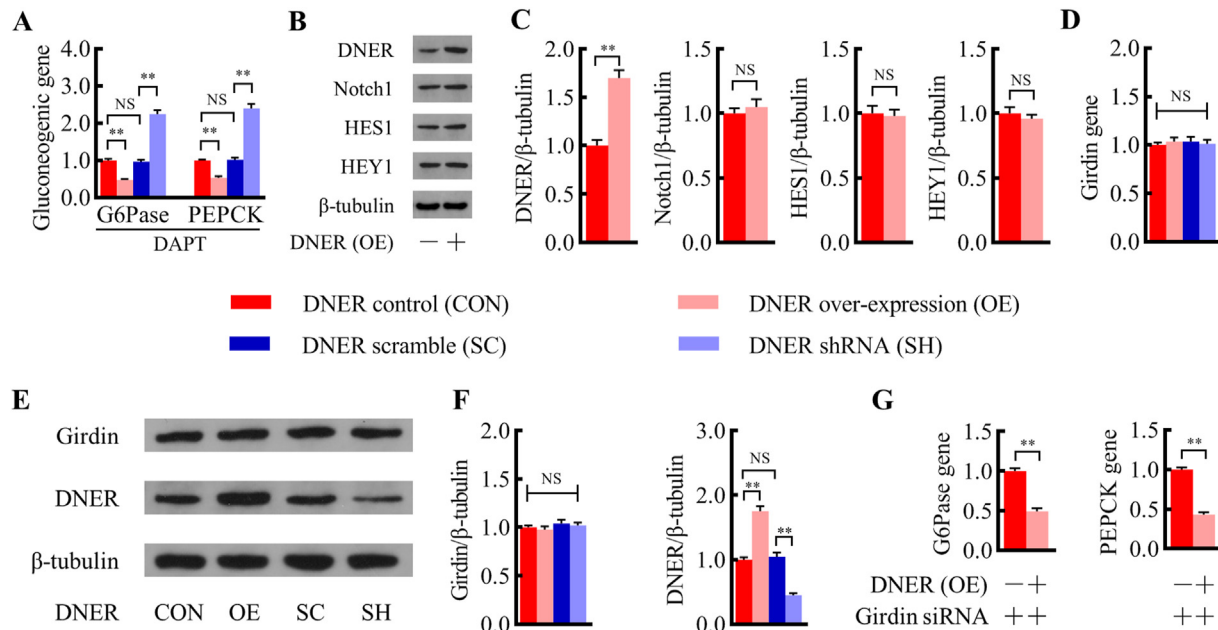
Figure 3: The effect of DNER on reducing hepatic gluconeogenic gene expression in AML-12 cells was independent of Notch1 and Girdin. (A) AML-12 cells with DNER over-expression or knockdown were treated with 20 μM DAPT for 12 h, followed with 100 nM insulin for 6 h. The mRNA expression of G6Pase and PEPCK induced by DNER over-expression or knockdown in the presence of DAPT were quantified by real-time PCR, with GAPDH serving as an internal control for normalization. (B–C) AML-12 cells transfected with a plasmid encoding an empty control vector or DNER were subjected to western blot analysis as indicated to detect the effect of DNER over-expression on Notch1 signaling pathway. (D–F) Effects of DNER over-expression or knockdown on the mRNA (D) and protein (E–F) level of Girdin. (G) The mRNA expression of G6Pase and PEPCK induced by DNER over-expression in the context of siRNA-induced Girdin gene silencing were quantified by real-time PCR, with GAPDH serving as an internal control. Data were normalized to control (CON group) and expressed as mean ± SE. n = 3. **, p < 0.01; NS, not statistically significant. CON, DNER empty control vector group; OE, DNER over-expression group; SC, DNER scramble group; SH, DNER shRNA group.

impaired insulin signaling in hepatic gluconeogenesis induced by DNER over-expression or knockdown can be rescued by TRB3 over-expression or knockdown, respectively (Figure 4A–D). These results suggested that TRB3 is required for DNER-mediated Akt phosphorylation and hepatic gluconeogenic gene expression.

Insulin induces Akt activation by stimulating tyrosine phosphorylation of insulin receptor, which in turn triggers activation of PI3K and PDK1. While we found that knockdown of DNER impaired insulin-stimulated Akt activation, it had no effect on phosphorylation of insulin receptor and PDK1 *in vitro* or *in vivo* (Figure 2A, B, G and H). We next investigated the role of Akt in mediating DNER action on hepatic gluconeogenesis using western blot analysis and quantitative real-time PCR in AML-12 cells transfected with a plasmid encoding DNER or an empty vector, and pretreated with or without 100 nM wortmannin for 15 min, then stimulated with 100 nM insulin for 10 min or 6 h. Over-expression of DNER enhanced insulin-stimulated activation of Akt (Figure 4E,F) and suppression of gluconeogenic genes expression (Figure 4G). Noticeably, wortmannin, an inhibitor of PI3K, the Akt upstream molecule, significantly diminished the potentiating effect of DNER over-expression on hepatic insulin signaling (Figure 4E–G). By contrast, SC79, an Akt phosphorylation activator, rescued the impaired insulin signaling in hepatic gluconeogenesis induced by DNER knockdown, as evaluated by Akt phosphorylation and hepatic gluconeogenic gene expression (Figure 4H–J). Given the previous finding that TRB3 binds to Akt and prevents insulin-mediated Akt activation by its upstream kinases [14], and the fact that knockdown of DNER had no significant effect on the protein abundance or phosphorylation of either the insulin receptor or PDK1 (Figure 2A, B, G and H), these results suggest that DNER enhances insulin-stimulated Akt activation but does not affect insulin-evoked signaling events upstream of Akt.

Taken together, these data indicate that DNER negatively regulates hepatic gluconeogenesis via a TRB3-Akt-dependent pathway.

3.5. DNER physically interacts with TRB3, and induces TRB3 UPS-dependent degradation

To further characterize the interaction between DNER and TRB3 proteins, we performed Co-IP experiments in AML-12 cells transfected with DNER and stimulated with or without 100 nM insulin for 10 min or 6 h, in the presence or absence of 10 μM MG132 for 6 h (Figure 5A). The results showed that there was an interaction between DNER and TRB3 under basal and insulin/MG132-stimulated conditions. Immunofluorescence studies also detected the association of DNER with TRB3 under basal and insulin-stimulated conditions, and the interaction was enhanced in AML-12 cells stimulated with insulin (Figure 5B). A cellular fractionation study was performed (Figure 6C) to analyze the localization of DNER and TRB3 in AML-12 hepatocytes. The western blot analysis of the fractions showed that DNER is mainly present at the membrane and TRB3 is mainly present in the nucleus without insulin stimulation. However, upon insulin stimulation, the levels of DNER and TRB3 in the cytoplasm significantly increased, demonstrating their interaction in the cytoplasm. To further confirm the above findings, we examined the interaction between DNER and TRB3 in C57BL/6J mice with or without hepatic DNER knockdown (Supplementary Figures 9 and 10). These Co-IP and immunofluorescence experiments suggested that interaction of DNER and TRB3 occurs *in vitro* and *in vivo*.

The shRNA-mediated reduction of DNER had entirely different effects on TRB3 protein and mRNA expression (Figure 2A–C, G–I), suggesting that DNER may regulate the stability of TRB3 protein. To test the hypothesis that DNER promotes TRB3 degradation, AML-12 cells were transfected with TRB3 together with HA-tagged empty vector or HA-
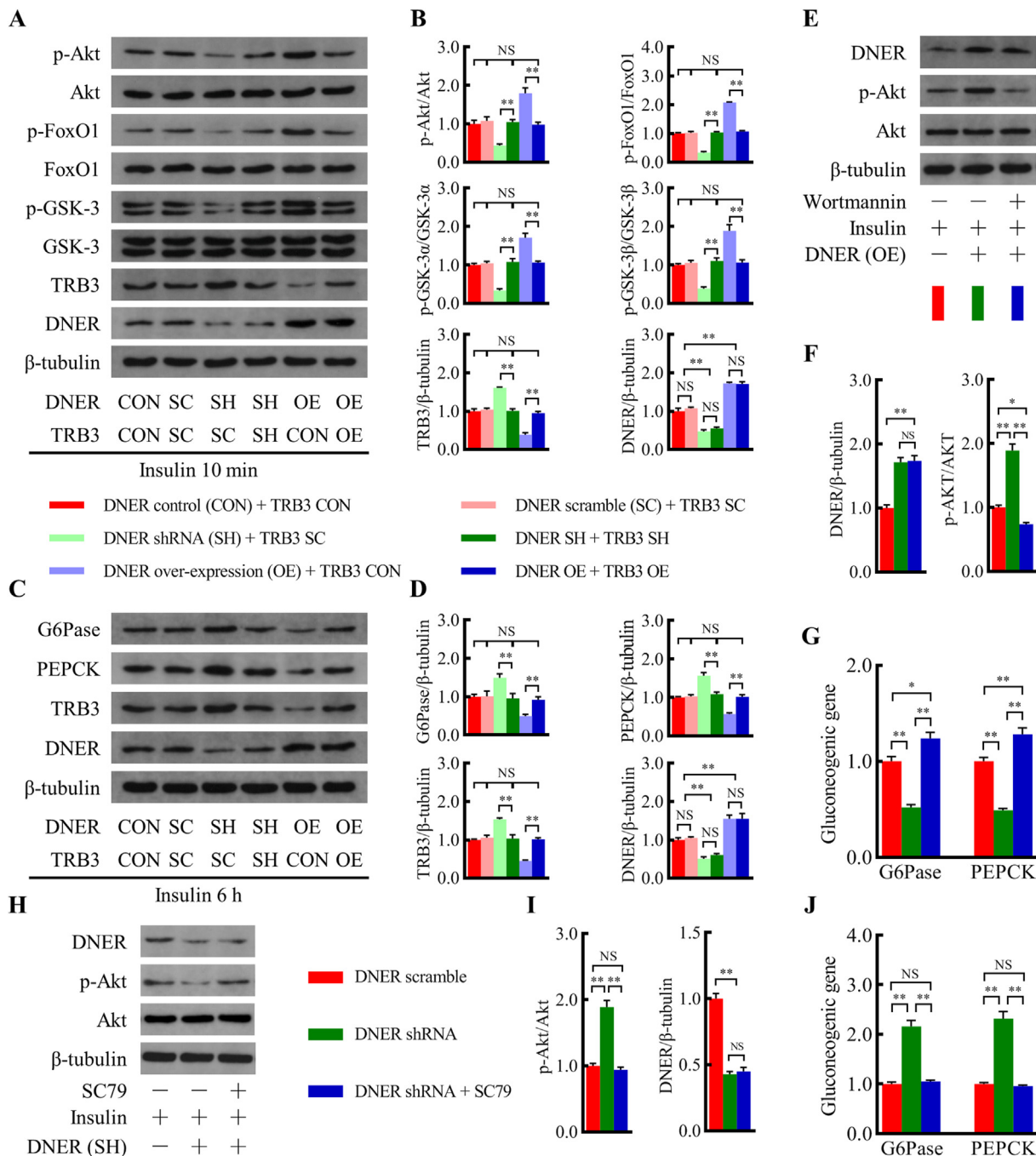
Figure 4: The inhibitory effect of DNER on gluconeogenesis is TRB3-Akt dependent. (A—D) AML-12 cells with DNER and/or TRB3 over-expression or knockdown were treated with 100 nM insulin for 10 min (A—B) or 6 h (C—D). Cell lysates were subjected to western blot analysis using antibodies as indicated. (E—G) AML-12 cells transfected with a plasmid encoding an empty control vector or DNER were pretreated with or without 100 nM wortmannin for 15 min, then stimulated with 100 nM insulin for 10 min (E—F) or 6 h (G). (E—F) Total cell lysates were subjected to western blot analysis using antibodies as indicated. (G) The mRNA expression of PEPCK and G6Pase were quantified by real-time PCR, with GAPDH serving as an internal control for normalization. (H—J) AML-12 cells transfected with adenovirus encoding DNER-specific shRNA or scrambled control were pretreated with or without 10 μM SC79 for 2 h, then stimulated with 100 nM insulin for 10 min (H—I) or 6 h (J). (H—I) Total cell lysates were subjected to western blot analysis using antibodies as indicated. (J) The mRNA expression of PEPCK and G6Pase were quantified by real-time PCR, with GAPDH serving as an internal control. Data were normalized to control and expressed as mean ± SE. n = 3. *, $p < 0.05$; **, $p < 0.01$; NS, not statistically significant. CON, empty control vector group; OE, over-expression group; SC, scramble group; SH, shRNA group.

tagged DNER, and treated with 100 μg/ml cycloheximide (CHX), a protein synthesis inhibitor (Figure 5C,D). When cells were treated with CHX, the turnover of TRB3 was accelerated by co-expression of DNER (Figure 5C,D). These results demonstrated that DNER could increase TRB3 turnover.

It is the proteasome inhibitor MG132 but not the autophagy inhibitor BFA that can abolish the decrease in TRB3 by DNER, indicating that downregulation of TRB3 by DNER occurs through proteasome pathway (Figure 5E,F). Consistent with this observation, neither over-expression of DNER *in vitro* (Figure 5E,F) nor knockdown of DNER *in vivo*
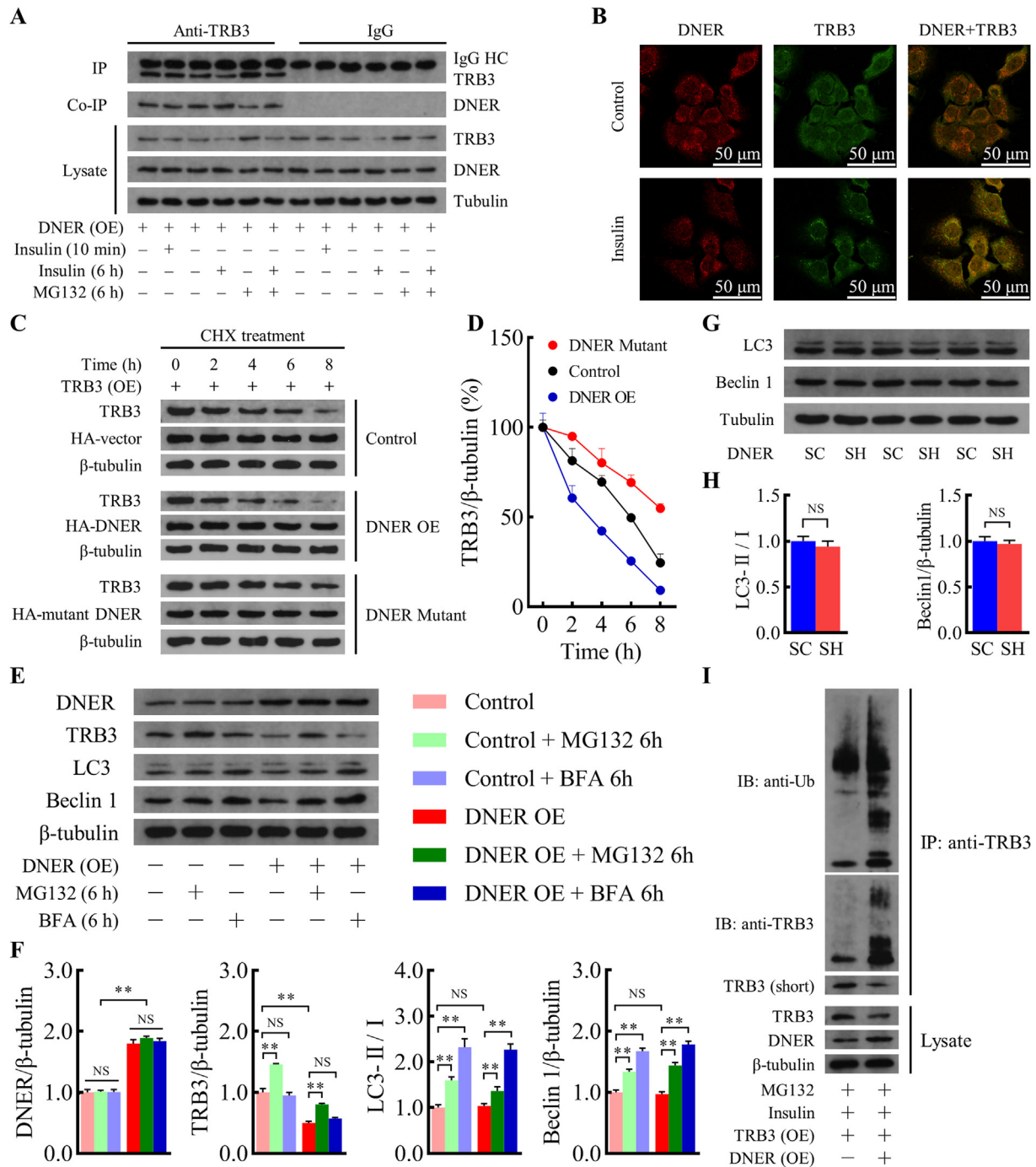
Figure 5: DNER interacts with TRB3 and mediates ubiquitin-proteasomal degradation of TRB3. (A) AML-12 cells over-expressing DNER were stimulated by 100 nM insulin for 10 min or 6 h, in the presence or absence of 10 μM MG132 for 6 h. Endogenous TRB3 was immunoprecipitated, and coimmunoprecipitated endogenous DNER was detected by western blot analysis. IgG HC, IgG heavy chain. (B) AML-12 cells over-expressing HA-tagged DNER were treated with culture medium alone (Control group) or with 100 nM insulin (Insulin group) for 10 min. Cells were fixed and stained with anti-HA or anti-TRB3, and examined by fluorescence microscopy. (C−D) AML-12 cells co-transfected with TRB3 and HA-tagged DNER empty control vector (Control group), HA-tagged DNER (DNER OE group) or HA-tagged point (Tyr^{677} to Ala) mutant DNER (DNER Mutant group) as indicated were treated with 100 μg/ml CHX and harvested at indicated times. The amount of TRB3 and HA were detected by western blot analysis with the specific antibodies indicated. n = 3. (E−F) AML-12 cells transfected with a plasmid encoding DNER (DNER OE) or an empty control vector (Control) were treated with culture medium alone, 10 μM MG132 or 100 nM BFA for 6 h. Cell lysates were subjected to western blot analysis to measure the protein levels of DNER, TRB3, LC3 and Beclin 1. n = 3. (G−H) C57BL/6J mice were treated with adenoviruses encoding DNER shRNA (SH group) or scrambled control (SC group) by two tail-vein injection. Liver tissues of mice were harvested and subjected to western blot analysis to measure the protein levels of LC3 and Beclin 1. n = 3. (I) A plasmid encoding DNER or an empty vector control were co-transfected into AML-12 cells over-expressing TRB3. Cells were stimulated by 100 nM insulin for 6 h, in the presence of 10 μM MG132, and subjected to immunoprecipitation with anti-TRB3 antibody. IP products were detected by western blot analysis using anti-Ub and anti-TRB3 antibodies. Data were expressed as percent variation of baseline (D) or were normalized to control (H and F), and presented as mean ± SE. **, $p < 0.01$; NS, not statistically significant.
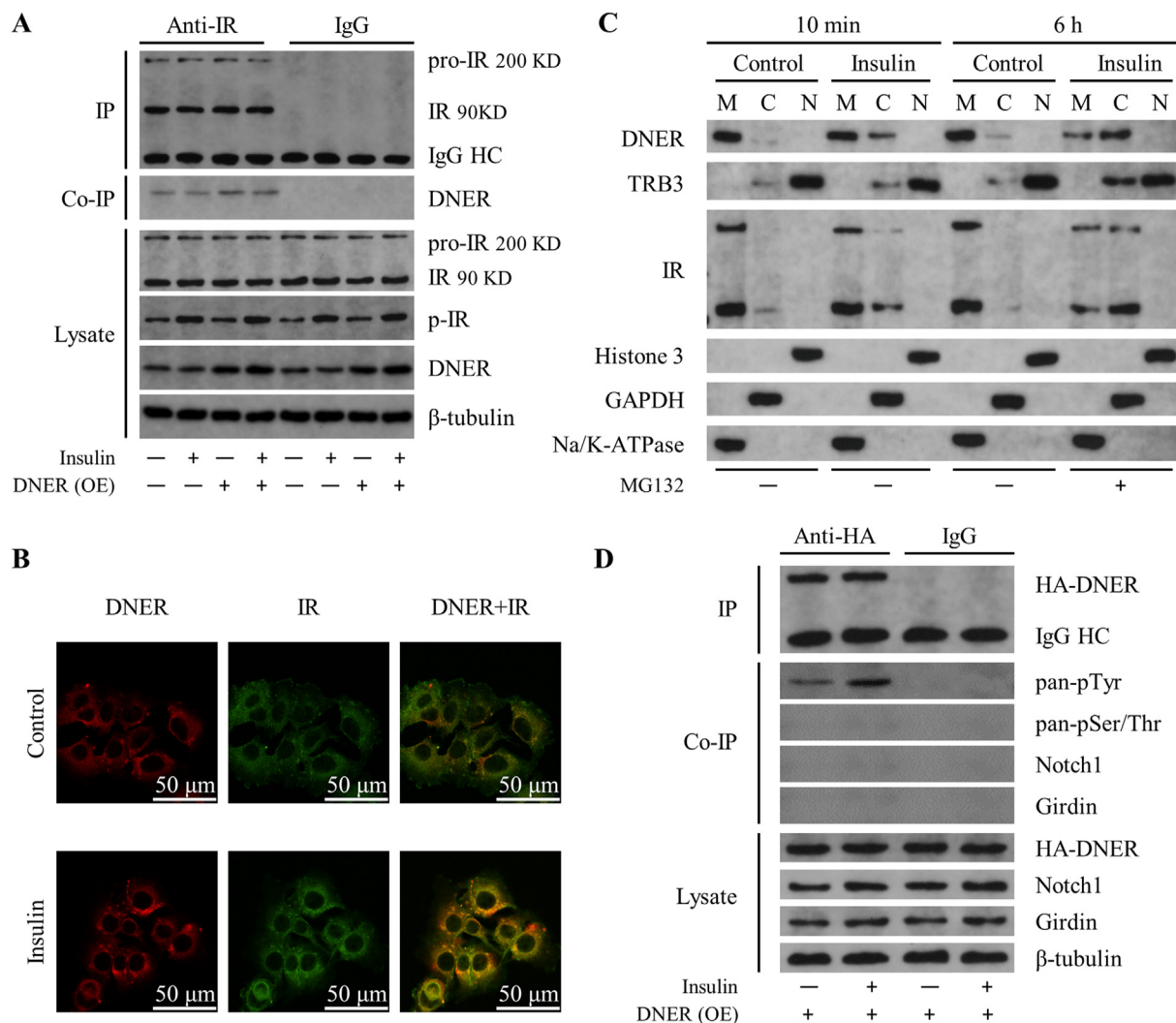
Figure 6: DNER interacts with insulin receptor and is tyrosine phosphorylated. (A) AML-12 cells transfected with a plasmid encoding DNER or an empty control vector were stimulated with or without 100 nM insulin for 10 min, and subjected to immunoprecipitation with anti-insulin receptor antibody. IP products were detected by western blot analysis using anti-insulin receptor and anti-DNER antibodies. (B) AML-12 cells over-expressing HA-tagged DNER were treated with culture medium alone (Control group) or with 100 nM insulin (Insulin group) for 10 min. Cells were fixed and stained with anti-HA or anti-insulin receptor, and examined by fluorescence microscopy. (C) AML-12 cells were stimulated with culture medium alone (Control group) or with 100 nM insulin (Insulin group) for 10 min or 6 h, in the presence or absence of 10 μM MG132 for 6 h. The subcellular location (M, membrane; C, cytoplasm; N, nuclear) of DNER, TRB3 and IR was analyzed by cell fractionation assay. (D) AML-12 cells over-expressing HA-tagged DNER were treated with culture medium alone or with 100 nM insulin for 10 min, and subjected to immunoprecipitation with anti-HA antibody. IP products were detected by western blot analysis using anti-HA, anti-Phospho-Tyrosine, anti-Phospho-Serine/Threonine, anti-Notch1 and anti-Girdin antibodies. IR, insulin receptor; p-IR, phosphorylated IR; IgG HC, IgG heavy chain. DNER (OE) −, DNER empty control vector group; DNER (OE) +, DNER over-expression group.

(Figure 5G,H) affected levels of autophagic markers including Beclin 1, LC3 and the ratio of LC3-II to LC3-I, suggesting that DNER contributes to TRB3 degradation independently of autophagy.

To further analyze the role of DNER in the degradation of TRB3, we conducted Co-IP experiments to detect DNER-mediated ubiquitination of TRB3 (Figure 5I). AML-12 cells were transfected with TRB3 together with DNER or empty control vector, treated with MG132 to prevent degradation of the ubiquitinated protein, stimulated by insulin, and subjected to IP with anti-TRB3 antibody. IP products were then detected by western blot using anti-Ub and anti-TRB3 antibodies. The results showed that a proportion of TRB3 was conjugated to ubiquitin and transfection of DNER increased TRB3 ubiquitination (Figure 5I). These results, collectively, demonstrated that DNER targets TRB3 for ubiquitin-proteasome system (UPS)-dependent degradation.

3.6. DNER physically interacts with insulin receptor, and is phosphorylated at Tyr^{677} in response to insulin stimulation

To investigate whether DNER potentiates insulin signaling by physically interacting with insulin receptor, we performed Co-IP experiments in AML-12 cells transfected with DNER or an empty control vector, and stimulated with or without 100 nM insulin for 10 min. These results showed that there was an interaction between DNER and insulin receptor under basal and insulin-stimulated conditions (Figure 6A). Immunofluorescence studies also supported the association of DNER with insulin receptor, especially in AML-12 cells stimulated with insulin (Figure 6B). A cellular fractionation study was conducted (Figure 6C) to analyze the localization of DNER and insulin receptor in AML-12 hepatocytes. The western blot analysis of the fractions revealed that under basal conditions, DNER and insulin

9

receptor were primarily present at the membrane. However, when stimulated with insulin, the levels of both DNER and insulin receptor in the cytoplasm significantly increased, demonstrating their interaction in the cytoplasm. To further confirm the above findings, we examined the interaction between DNER and insulin receptor in C57BL/6J mice with or without hepatic DNER knockdown (Supplementary Figures 11 and 12). These Co-IP and immunofluorescence experiments suggested that interaction of DNER and insulin receptor occurs in vitro and in vivo.

DNER contains several potential phosphorylation modification sites, especially a tyrosine-based sorting motif in its cytoplasmic domain which is required for dendritic targeting of DNER in central nervous system [17]. To investigate the potential role of DNER phosphorylation, we performed Co-IP experiments in AML-12 cells transfected with HA-tagged DNER. After stimulated with or without 100 nM insulin for 10 min, AML-12 cells were collected. Then complexes were immunoprecipitated with anti-HA-conjugated agarose beads and detected by western blot with antibodies against HA, phospho-Tyrosine, and phospho-Serine/Threonine. Insulin treatment significantly stimulated the phosphorylation of DNER at tyrosine rather than serine or threonine (Figure 6D).

To locate the exact phospho-tyrosine modification sites, AML-12 cells over-expressed with HA-tagged DNER were stimulated with or without 100 nM insulin for 10 min, then were lysed and immunoprecipitated with anti-HA-conjugated agarose beads and subjected to LC-MS/MS analysis. Among the four (Tyr^{677}, Tyr^{711}, Tyr^{640} and Tyr^{543}) potential tyrosine phosphorylation sites identified by mass spectrometry, Tyr^{711} and Tyr^{640} were firstly excluded since the peptide intensity of these two sites in the non-insulin-stimulated group was higher than that in the insulin-stimulated group (Supplementary Table 3). Tyr^{677} was the only phosphorylation site not found in any of the triplicate non-insulin-stimulated group samples, while it was observed twice in the triplicate insulin-stimulated group samples (Supplementary Table 3; Supplementary Figures 13A—D).

Together, these results indicated that DNER can interact with insulin receptor. Instead of serine or threonine, DNER is phosphorylated at tyrosine in response to insulin stimulation, and Tyr^{677} is the potential phosphorylation site.

3.7. Tyr^{677} phosphorylation is essential for DNER to potentiate insulin-stimulated activation of Akt and suppression of gluconeogenesis in AML-12 hepatocytes

To determine the role of Tyr^{677} phosphorylation in mediating insulin sensitization by DNER, we over-expressed the HA-tagged wild-type and mutant (Tyr^{677} to Ala) DNER in AML-12 hepatocytes.

Neither DNER mutation (Figure 7E) nor knockdown (Figure 2C,I) affected the gene expression level of TRB3, providing additional evidence that DNER regulates TRB3 at the protein level, rather than the gene level.

Of note, replacing tyrosine with alanine greatly impaired phosphorylation of DNER in response to insulin stimulation (Figure 7A), concurrent with attenuated DNER-induced degradation of TRB3 (Figures 5C,D and 7B,C). Consequently, the potentiating effect of DNER on insulin-stimulated activation of Akt and suppression of gluconeogenic genes (G6Pase and PEPCK) expression were significantly reduced by mutating Tyr^{677} of DNER to Ala (Figure 7B—D). These changes were accompanied by reduced phosphorylation of FoxO1 and GSK3α/β (Figure 7B,C), decreased 2-DG uptake (Figure 7F) and increased glucose production (Figure 7G). Taken together, these results clearly demonstrate that phosphorylation at Tyr^{677} plays a key role in potentiating hepatic insulin signaling in gluconeogenesis.

4. DISCUSSION

Gluconeogenesis is a major contributor to half of the total HGP in individuals following an overnight fast and is primarily responsible for the fasting hyperglycemia in patients with T2DM [1—3]. The absence of a curative therapy for the abnormally increased hepatic gluconeogenesis make necessary the exploration of new targets. In this study, we provide initial evidence supporting the fundamental role of DNER in hepatic gluconeogenesis. We found that the protein level of DNER in liver of ob/ob and db/db mice are obviously lower than that of C57BL/6J control mice, and that lower DNER protein level is associated with lower Akt activity. Furthermore, hepatic DNER knockdown not only significantly attenuated Akt activity and then upregulated gluconeogenic gene (G6Pase and PEPCK) expression in AML-12 hepatocytes and in C57BL/6J mice, but also resulted in impaired glucose and pyruvate tolerance in C57BL/6J mice. On the contrary, DNER over-expression enhanced Akt activity and then downregulated G6Pase and PEPCK levels in AML-12 hepatocytes, by interacting with TRB3 directly and inducing TRB3 UPS-dependent degradation. In addition, we demonstrated that in response to insulin stimulation, DNER interacted directly with insulin receptor and was phosphorylated at Tyr^{677}, and this site-specific phosphorylation is essential for DNER-mediated hepatic gluconeogenesis. Our study thus reveals a mechanism underlying the role of DNER in inhibiting hepatic gluconeogenesis and sensitizing insulin-stimulated Akt pathway.

Although DNER lacks the Delta/Serrate/Lag (DSL) binding domain [5] which regarded as essential for Notch ligand [18,19], it has been explored as a non-canonical Notch ligand binding to the Notch1 receptor in Purkinje neurons [5], C2C12 myoblasts [5], glioblastoma-derived neoplastic stem-like cells [8] and prostate cancer cells [20]. Notch1 has been reported as a regulator of hepatic G6Pase gene expression [12,13]. However, no association between DNER and Notch signaling was observed in human adipose tissue-derived mesenchymal stem cells [6] or in MDA-MB-231 human breast cancer cells [9]. In addition, DNER exerts tumor-promoting effects in breast cancer [9] and hepatocellular carcinoma [21], but possesses tumor-suppressive effects in glioblastoma [8]. These inconsistent or contrary results suggest that the role of DNER is tissue- or cell-specific. Our results in AML-12 hepatocytes showed that DNER could neither regulate the expression of Notch1 nor the expression of Notch signal proteins such as HES1 and HEY1, and the inhibition of DNER on G6Pase and PEPCK gene expression could not be reversed by DAPT, a specific inhibitor of Notch signaling pathway. Furthermore, no interaction between DNER and Notch1 was observed in Co-IP experiments. Hence, DNER negatively regulated hepatic gluconeogenesis in a Notch1-independent manner.

Girdin, also named Gα-interacting vesicle-associated protein (GIV), was identified as an actin-binding Akt substrate that increases insulin sensitivity in myoblast cells through upregulating Akt and insulin receptor substrate-1 phosphorylation [22] and is required for insulin signaling in cell wound repair [23]. Recently, we have shown that the tyrosine-based sorting motif of DNER could be phosphorylated in response to pleiotrophin stimulation, then interacted with Girdin to further activate PI3K/Akt signaling pathway, resulting in breast cancer cells proliferation and metastasis [9]. In this study, adenovirus-mediated over-expression or knockdown of DNER did not alter the protein abundance of Girdin. Moreover, Co-IP analysis did not detect the association between DNER and Girdin. Knockdown of Girdin in AML-12 hepatocytes did not negate the effects of DNER on gluconeogenic gene expression in response to insulin stimulation, while the PI3K inhibitor wortmannin did. Interestingly, SC79, an Akt
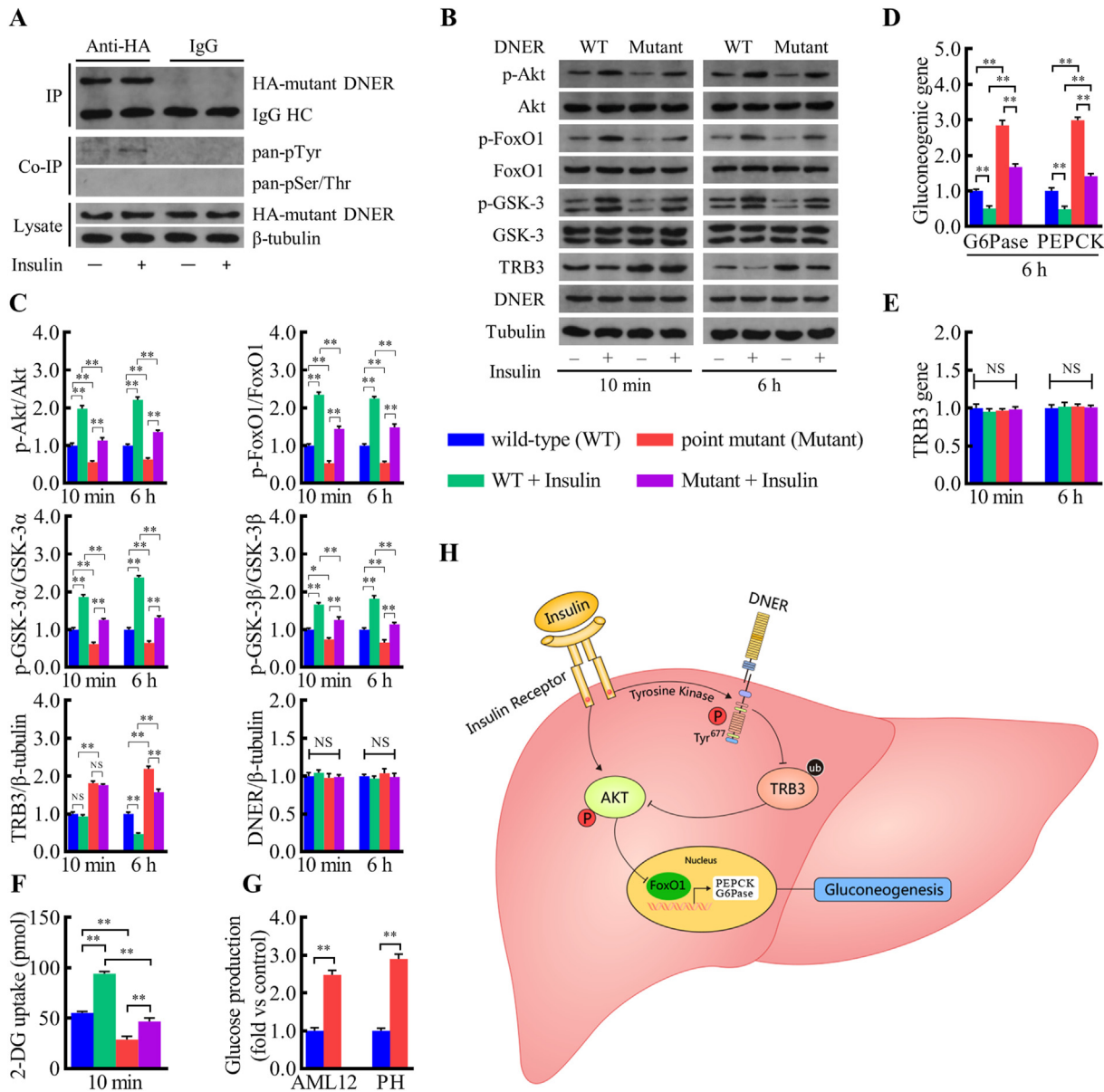
Figure 7: Tyr[677] phosphorylation is essential for the promoting effect of DNER on insulin signaling. (A) AML-12 cells over-expressing HA-tagged point mutant (Tyr[677] to Ala) DNER were treated with culture medium alone or with 100 nM insulin for 10 min, and subjected to immunoprecipitation with anti-HA antibody. IP products were detected by western blot analysis using anti-HA, anti-Phospho-Tyrosine and anti-Phospho-Serine/Threonine antibodies. IgG HC, IgG heavy chain. (B−F) AML-12 cells transfected with a plasmid encoding wild-type DNER (WT group) or point mutant (Tyr[677] to Ala) DNER (Mutant group) were stimulated with or without 100 nM insulin for 10 min or 6 h. (B−C) Total cell lysates were subjected to western blot analysis using antibodies as indicated. (D−E) The mRNA expression of G6Pase, PEPCK (D) and TRB3 (E) were quantified by real-time PCR, with GAPDH serving as an internal control for normalization. (F) Glucose uptake was determined using 2-DG absorbance in AML-12 cells transfected with a plasmid encoding wild-type DNER (WT group) or point mutant (Tyr[677] to Ala) DNER (Mutant group). (G) Glucose output assay was performed in AML-12 cells and primary mouse hepatocytes (PH) transfected with adenovirus encoding wild-type DNER (WT group) or point mutant (Tyr[677] to Ala) DNER (Mutant group). (H) Schematic of tyrosine-phosphorylated DNER sensitizing insulin signaling in hepatic gluconeogenesis by inducing ubiquitin-proteasomal degradation of TRB3. n = 4. Data were normalized to control (WT group; C, D, E and G) and expressed as mean ± SE. *, $p < 0.05$; **, $p < 0.01$; NS, not statistically significant.

phosphorylation activator, rescued the impaired insulin signaling induced by DNER knockdown. Collectively, these results in our study suggest that DNER regulates hepatic gluconeogenesis through an unrecognized Akt-dependent pathway other than Girdin.

TRB3 has been well-characterized as a negative modulator of insulin signaling, binding directly to Akt and blocking Akt phosphorylation [14]. Knockdown of hepatic TRB3 expression in mice improved glucose tolerance and insulin sensitivity, whereas over-expression of TRB3 resulted in glucose intolerance and insulin resistance [14,24]. In the present study, we found that the protein level of TRB3 in insulin target tissues such as liver, skeletal muscle and epididymal fat of C57BL/6J mice was significantly lower than that of age- and gender-matched *ob/ob* and *db/db* mice; on the contrary, the DNER protein level and Akt activity in C57BL/6J mice were higher than those in *ob/ob* and *db/db* mice. Moreover, we demonstrated that TRB3 is required for DNER-regulated Akt phosphorylation and hepatic gluconeogenic gene expression. In support of this notion, the impaired or improved insulin signaling in hepatic gluconeogenesis induced by DNER knockdown or

over-expression in our study can be rescued by TRB3 knockdown or over-expression, respectively. Our observations that in AML-12 hepatocytes, DNER physically interacts with TRB3 and regulates the stability of TRB3 via the UPS degradation pathway, consistent with previous studies [25,26] providing additional evidence that TRB3 is an unstable protein and its steady-state levels are balanced through proteasome-dependent degradation. Therefore, the potentiating effect of DNER on insulin-stimulated suppression of hepatic gluconeogenesis can be attributed to its ability in counteracting the inhibition of Akt activation by TRB3.

Insulin receptor is a heterotetrameric receptor composed of two extracellular α-subunits with insulin-binding site, and two membrane-spanning β-subunits with cytoplasmic tyrosine kinase catalytic domain [2]. Insulin exerts its physiological effects by binding to the α-subunit and activating autophosphorylation of the β-subunit, which in turn phosphorylates various insulin receptor substrate proteins [2,3]. Interestingly, DNER is a single-pass transmembrane protein containing multiple function domains including ten extracellular EGF-like motifs and one intracellular tyrosine-based sorting motif [17]. This raised an intriguing possibility that the tyrosine-based sorting motif might be a potential phosphorylation site by tyrosine kinases of insulin receptor. Our results demonstrated that in response to insulin stimulation, DNER interacted directly with insulin receptor and was phosphorylated on tyrosine. To better understand the role of the phosphorylated DNER in sensitizing the insulin signaling, we searched for phosphorylated modification on DNER by using mass spectrometry, and found that point mutation in the tyrosine-based sorting motif (Tyr^{677} to Ala) significantly disrupted the effects of DNER on Akt activation and hepatic gluconeogenesis. These results strongly support the idea that insulin receptor recognizes and phosphorylates the tyrosine-based sorting motif in the DNER cytoplasmic tail, which is required for DNER to upregulate Akt activity and inhibit hepatic gluconeogenesis.

5. CONCLUSIONS

Overall, our study revealed a novel role of DNER in potentiating insulin-stimulated activation of Akt and suppression of gluconeogenesis in hepatocytes. In addition, we demonstrated that DNER phosphorylation at Tyr^{677}, which is stimulated by insulin, plays a key role in inducing proteasomal degradation of TRB3 and inhibiting hepatic gluconeogenesis through the Akt-FoxO1-G6Pase/PEPCK pathway. The finding that Tyr^{677} phosphorylation is stimulated by insulin also uncovers a mechanism underlying the crosstalk between the DNER- and insulin-signaling pathways.

CREDIT AUTHORSHIP CONTRIBUTION STATEMENT

Junfeng Li: Writing — review & editing, Writing — original draft, Validation, Methodology, Investigation, Funding acquisition, Formal analysis, Data curation, Conceptualization. **Yan Huang:** Formal analysis, Data curation. **Xinyu Yang:** Formal analysis, Data curation. **Yuli Cai:** Formal analysis, Data curation. **Ye Wang:** Formal analysis, Data curation. **Wenling Dai:** Formal analysis, Data curation. **Liu Jiang:** Formal analysis, Data curation. **Changhua Wang:** Writing — original draft, Supervision, Funding acquisition, Conceptualization. **Zhongyuan Wen:** Writing — original draft, Supervision, Conceptualization.

DECLARATION OF COMPETING INTEREST

The authors declare that they have no known competing financial interests or personal relationships that could have appeared to influence the work reported in this paper.

DATA AVAILABILITY

Data will be made available on request.

ABBREVIATIONS

T2DM	type 2 diabetes mellitus
DNER	Delta/Notch-like epidermal growth factor (EGF)-related receptor
TRB3	tribbles homolog 3
G6Pase	glucose-6-phosphatase
PEPCK	phosphoenolpyruvate carboxykinase
PI3K	phosphoinositide 3-kinase
FoxO1	Forkhead box O1
shRNA	short hairpin RNA
Co-IP	Co-immunoprecipitation
OGTT	oral glucose tolerance test
PTT	pyruvate tolerance test
BFA	Bafilomycin A1
CHX	cycloheximide
UPS	ubiquitin-proteasome system

APPENDIX A. SUPPLEMENTARY DATA

Supplementary data to this article can be found online at https://doi.org/10.1016/j.molmet.2024.101927.

REFERENCES

[1] Titchenell PM, Lazar MA, Birnbaum MJ. Unraveling the regulation of hepatic metabolism by insulin. Trends Endocrinol Metab Trends Endocrinol Metab 2017;28:497—505.

[2] Petersen MC, Shulman GI. Mechanisms of insulin action and insulin resistance. Physiol Rev 2018;98:2133—223.

[3] Hatting M, Tavares CDJ, Sharabi K, Rines AK, Puigserver P. Insulin regulation of gluconeogenesis. Ann N Y Acad Sci 2018;1411:21—35.

[4] American Diabetes Association Professional Practice C, Draznin B, Aroda VR, Bakris G, Benson G, Brown FM, et al. 9. Pharmacologic approaches to glycemic treatment: standards of medical care in diabetes-2022. Diabetes Care 2022;45:S125—43.

[5] Eiraku M, Tohgo A, Ono K, Kaneko M, Fujishima K, Hirano T, et al. DNER acts as a neuron-specific Notch ligand during Bergmann glial development. Nat Neurosci 2005;8:873—80.

[6] Park JR, Jung JW, Seo MS, Kang SK, Lee YS, Kang KS. DNER modulates adipogenesis of human adipose tissue-derived mesenchymal stem cells via regulation of cell proliferation. Cell Prolif 2010;43:19—28.

[7] Hartman BH, Nelson BR, Reh TA, Bermingham-McDonogh O. Delta/notch-like EGF-related receptor (DNER) is expressed in hair cells and neurons in the

developing and adult mouse inner ear. J Assoc Res Otolaryngol 2010;11:187—201.

[8] Sun P, Xia S, Lal B, Eberhart CG, Quinones-Hinojosa A, Maciaczyk J, et al. DNER, an epigenetically modulated gene, regulates glioblastoma-derived neurosphere cell differentiation and tumor propagation. Stem Cells 2009;27: 1473—86.

[9] Wang L, Wu Q, Li Z, Sun S, Yuan J, Li J, et al. Delta/notch-like epidermal growth factor-related receptor promotes stemness to facilitate breast cancer progression. Cell Signal 2019;63:109389.

[10] Hanson RL, Muller YL, Kobes S, Guo T, Bian L, Ossowski V, et al. A genome-wide association study in American Indians implicates DNER as a susceptibility locus for type 2 diabetes. Diabetes 2014;63:369—76.

[11] Deng Z, Shen J, Ye J, Shu Q, Zhao J, Fang M, et al. Association between single nucleotide polymorphisms of delta/notch-like epidermal growth factor (EGF)-related receptor (DNER) and Delta-like 1 Ligand (DLL 1) with the risk of type 2 diabetes mellitus in a Chinese Han population. Cell Biochem Biophys 2015;71:331—5.

[12] Pajvani UB, Shawber CJ, Samuel VT, Birkenfeld AL, Shulman GI, Kitajewski J, et al. Inhibition of Notch signaling ameliorates insulin resistance in a FoxO1-dependent manner. Nat Med 2011;17:961—7.

[13] Bernsmeier C, Dill MT, Provenzano A, Makowska Z, Krol I, Muscogiuri G, et al. Hepatic Notch1 deletion predisposes to diabetes and steatosis via glucose-6-phosphatase and perilipin-5 upregulation. Lab Investig J Technol Methods Pathol 2016;96:972—80.

[14] Du K, Herzig S, Kulkarni RN, Montminy M. TRB3: a tribbles homolog that inhibits Akt/PKB activation by insulin in liver. Science 2003;300:1574—7.

[15] Charni-Natan M, Goldstein I. Protocol for primary mouse hepatocyte isolation. STAR Protoc 2020;1:100086.

[16] Li J, Wang Z, Ren L, Fan L, Liu W, Jiang Y, et al. Antagonistic interaction between Nodal and insulin modulates pancreatic beta-cell proliferation and survival. Cell Commun Signal 2018;16:79.

[17] Eiraku M, Hirata Y, Takeshima H, Hirano T, Kengaku M. Delta/notch-like epidermal growth factor (EGF)-related receptor, a novel EGF-like repeat-containing protein targeted to dendrites of developing and adult central nervous system neurons. J Biol Chem 2002;277:25400—7.

[18] Luca VC, Jude KM, Pierce NW, Nachury MV, Fischer S, Garcia KC. Structural biology. Structural basis for Notch1 engagement of Delta-like 4. Science 2015;347:847—53.

[19] Cordle J, Johnson S, Tay JZ, Roversi P, Wilkin MB, de Madrid BH, et al. A conserved face of the Jagged/Serrate DSL domain is involved in Notch trans-activation and cis-inhibition. Nat Struct Mol Biol 2008;15:849—57.

[20] Wang L, Wu Q, Zhu S, Li Z, Yuan J, Yu D, et al. Delta/notch-like epidermal growth factor-related receptor (DNER) orchestrates stemness and cancer progression in prostate cancer. Am J Transl Res 2017;9:5031—9.

[21] Liang Y, Luo H, Zhang H, Dong Y, Bao Y. Oncogene delta/notch-like EGF-related receptor promotes cell proliferation, invasion, and migration in hepatocellular carcinoma and predicts a poor prognosis. Cancer Biother Radiopharm 2018;33:380—6.

[22] Hartung A, Ordelheide AM, Staiger H, Melzer M, Haring HU, Lammers R. The Akt substrate Girdin is a regulator of insulin signaling in myoblast cells. Biochim Biophys Acta 2013;1833:2803—11.

[23] Nakamura M, Verboon JM, Allen TE, Abreu-Blanco MT, Liu R, Dominguez ANM, et al. Autocrine insulin pathway signaling regulates actin dynamics in cell wound repair. PLoS Genet 2020;16:e1009186.

[24] Koo SH, Satoh H, Herzig S, Lee CH, Hedrick S, Kulkarni R, et al. PGC-1 promotes insulin resistance in liver through PPAR-alpha-dependent induction of TRB-3. Nat Med 2004;10:530—4.

[25] Ohoka N, Sakai S, Onozaki K, Nakanishi M, Hayashi H. Anaphase-promoting complex/cyclosome-cdh1 mediates the ubiquitination and degradation of TRB3. Biochem Biophys Res Commun 2010;392:289—94.

[26] Zhou Y, Li L, Liu Q, Xing G, Kuai X, Sun J, et al. E3 ubiquitin ligase SIAH1 mediates ubiquitination and degradation of TRB3. Cell Signal 2008;20:942—8.